

Supplemental Material for

Room temperature ferromagnetism properties of $\text{Ga}_{14}\text{N}_{16-n}\text{Gd}_2\text{C}_n$ monolayers: A first principle study

Shijian Tian ¹, Libo Zhang ^{3,*}, Yuan Liang ^{1,*}, Ruikuan Xie ⁴, Li Han ³, Shiqi Lan ¹,
Aijiang Lu ¹, Yan Huang ^{2,*}, Huaizhong Xing ^{1,*}, Xiaoshuang Chen ²

¹*Department of Optoelectronic Science and Engineering, Donghua University, Shanghai 201620, China*

²*State Key Laboratory of Infrared Physics, Shanghai Institute of Technical Physics, Chinese Academy of Sciences, Shanghai 200083, China*

³*College of Physics and Optoelectronic Engineering, Hangzhou Institute for Advanced Study, University of Chinese Academy of Sciences, No. 1, Sub-Lane Xiangshan, Xihu District, Hangzhou 310024, China.*

⁴*State Key Laboratory of Structural Chemistry, Fujian Institute of Research on the Structure of Matter, Chinese Academy of Sciences (CAS), Fuzhou, 350002 Fujian, China.*

**Corresponding author*

Email: zhanglibo@ucas.ac.cn (L. B. Zhang)

Email: xinghz@dhu.edu.cn (H. Z. Xing).

Email: yliang@dhu.edu.cn (Y. Liang).

Email: yhuang@mail.sitp.ac.cn (Y. Huang).

To observe the effect of size, the band structures and PDOS of supercells $4 \times 4 \times 1$ ($\text{Ga}_{14}\text{N}_{16}\text{Gd}_2$), $5 \times 5 \times 1$ ($\text{Ga}_{23}\text{N}_{25}\text{Gd}_2$) and $6 \times 6 \times 1$ ($\text{Ga}_{34}\text{N}_{36}\text{Gd}_2$) are shown at Figure S1. It is found that the band structures are similar, the band gap values for the spin-up channels for the three sizes are 1.99 eV, 2.00 eV and 2.01 eV, respectively, while the spin-down channels are 2.05 eV, 2.07 eV, and 2.04 eV, respectively. For the three sizes of $\text{Ga}_{14}\text{N}_{16}\text{Gd}_2$ monolayers, the band structures of spin-up and spin-down channel are similar, with an almost equivalent band gap. The size effect has ignorable influence on the electronic and magnetic properties of the Gd-pair doped GaN monolayer.

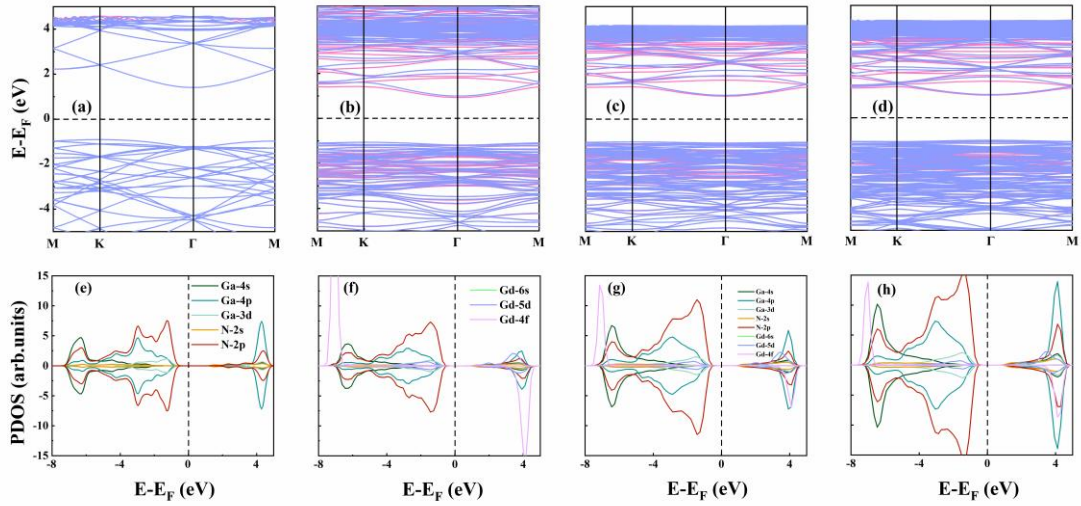


Figure S1. Band structures of (a) $\text{Ga}_{16}\text{N}_{16}$ (b) $\text{Ga}_{14}\text{N}_{16}\text{Gd}_2$, (c) $\text{Ga}_{23}\text{N}_{25}\text{Gd}_2$ and (d) $\text{Ga}_{34}\text{N}_{36}\text{Gd}_2$ monolayers. The blue and pink solid lines in the band structure represent spin up and spin down channels, respectively. PDOS of (e) $\text{Ga}_{16}\text{N}_{16}$ (f) $\text{Ga}_{14}\text{N}_{16}\text{Gd}_2$, (g) $\text{Ga}_{23}\text{N}_{25}\text{Gd}_2$ and (h) $\text{Ga}_{34}\text{N}_{36}\text{Gd}_2$ monolayers. The dash lines present the fermi-level which is taken to be 0.

The magnetic coupling between Gd and C atoms are studied by mapping the total energy to the classical Heisenberg model. The nearest-neighboring exchange coupling is considered to associated with the magnetic phase and label it as J . The Hamiltonian can be defined as:

$$H = -J_1 \sum_{\langle i, j \rangle} S_i S_j \quad 1$$

In the formula, S is the spin vector; $\langle i, j \rangle$ is summation over the nearest-neighboring Gd-pair. The energies of magnetic states can be described as:

$$E_{\text{FM}} = E_0 - 3JS^2, \quad E_{\text{AFM}} = E_0 + JS^2$$

E_0 is the reference energy. Thus, the magnetic coupling parameter (J) can be defined as:

$$J = (E_{\text{AFM}} - E_{\text{FM}}) / 4S^2 \quad 2$$

The corresponding atomic structure is shown at Figure 1, the positions of the C-atom doping are marked as the numbers inserted in Figure 1a. The E_b , ΔE , M_{total} , J [39] and T_C are studied by PBE method are shown at Table S1 and S2. It can be observed that the E_b and M_{total} of the FM phase are equivalent for a fixed C concentration, indicating that the substituted sites substitution has no impact on the structural stability and magnetic moment. However, the structural stability decreases with the increase of C concentration. **For example, when the C atom concentration reaches 12.5% (4 C atoms), the magnetic state is no more stable and the structural stability decreases by 16.49%.** It can be seen that the substitutional impurity of C atom has significant effect on the ground state of GaN: Gd monolayers, not all doping scheme maintain positive ΔE and J . The positive ΔE and J values indicate the FM phase, which is detected in the following configurations: [M], [1, 3], [M, 6], [M, 8], [2, 3, 5], [M, 5, 7] and [M, 5, 7, 8]. Negative values indicating AFM phases which are detected the following configurations: [1], [4], [5], [8], [1, 2], [5, 7], [M, 1], [M, 2], [1, 2, 3], [5, 6, 7], [1, M, 2], [1, M, 3], [2, M, 5] and [M, 4, 6, 7].

Table S1. The E_b of FM phase, total magnetic moments (M_{total}), ΔE ($E_{\text{AFM}}-E_{\text{FM}}$), nearest-neighboring exchange (J), estimated T_C^{FMA} and T_C of $\text{Ga}_{14}\text{N}_{16}\text{Gd}_2$, $\text{Ga}_{14}\text{N}_{15}\text{Gd}_2\text{C}_1$, $\text{Ga}_{14}\text{N}_{14}\text{Gd}_2\text{C}_2$, $\text{Ga}_{14}\text{N}_{13}\text{Gd}_2\text{C}_3$, $\text{Ga}_{14}\text{N}_{12}\text{Gd}_2\text{C}_4$, respectively.

	E_b (eV)	M_{total} (μ_B)	ΔE (meV)	J (meV)	T_C^{FMA} (K)	T_C (K)
$\text{Ga}_{14}\text{N}_{16}\text{Gd}_2$	-5.64	14.00	-4.08	-0.08	-	-
[1]	-5.56	15.00	-3.82	-0.08	-	-
[4]	-5.57	15.00	-10.26	-0.21	-	-
[5]	-5.57	15.00	-4.04	-0.08	-	-
[8]	-5.57	15.00	-1.90	-0.04	-	-
[M]	-5.54	15.00	15.05	0.31	58.22	35.51
[1, 2]	-5.48	16.00	-0.77	-0.02	-	-
[5, 7]	-5.50	16.00	-0.90	-0.02	-	-
[M, 1]	-5.47	16.00	-1767.19	-36.07	-	-
[M, 2]	-5.47	16.00	-1770.46	-36.13	-	-
[1, 3]	-5.48	16.00	14.77	0.30	57.13	34.85
[M, 6]	-5.48	16.00	14.14	0.29	54.70	33.36
[M, 8]	-5.48	16.00	111.81	2.26	428.63	261.46
[2, M, 5]	-5.08	17.00	-2222.17	-45.36	-	-
[1, M, 2]	-5.07	17.00	-2335.62	-47.67	-	-
[1, M, 3]	-5.08	17.00	-2409.58	-49.18	-	-
[1, 2, 3]	-5.09	17.00	-0.49	-0.01	-	-
[5, 6, 7]	-5.12	17.00	-61.21	-1.25	-	-
[2, 3, 5]	-5.10	17.00	51.26	1.05	198.28	120.95
[M, 5, 7]	-5.10	17.00	82.55	1.68	319.32	194.78
[M, 4, 6, 7]	-4.71	18.00	-3.34	-0.07	-	-
[M, 5, 7, 8]	-4.71	18.00	155.12	3.17	600.03	366.02

The PDOS of following examples are shown in Fig. S2, which are used to investigate the underlying mechanisms of the above phenomena: [1], [4], [M, 2], [5, 7], [2, M, 5] and [1, M, 2]. It is shown that one of the factors causing the negative ΔE and

J is due to the apparently weaker p-d coupling between the Gd-5d and C-2p states near the Fermi level ([1], [4] and [5, 7] in Figure S3). In addition, the energy of the AFM state of the special substitution site is reduced dramatically, resulting in AFM ground state, such as [M, 2], [2, M, 5], [1, M, 2] (shown in Figure S4). In summary, we define the ideal scheme with a stable FM phase and relatively high T_C : one C atoms at M positions and other C atoms bonded without Gd atoms: (M), (M, 8) and (M, 5, 7).

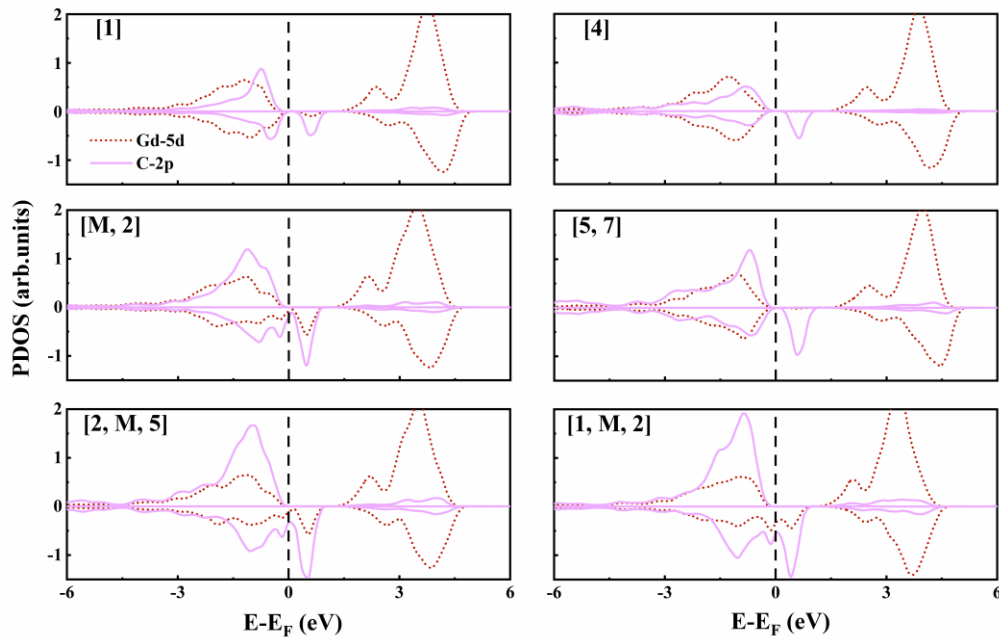


Figure S2. PDOS with FM states of different substitution site: [1], [4], [M, 2], [5, 7], [2, M, 5] and [1, M, 2].

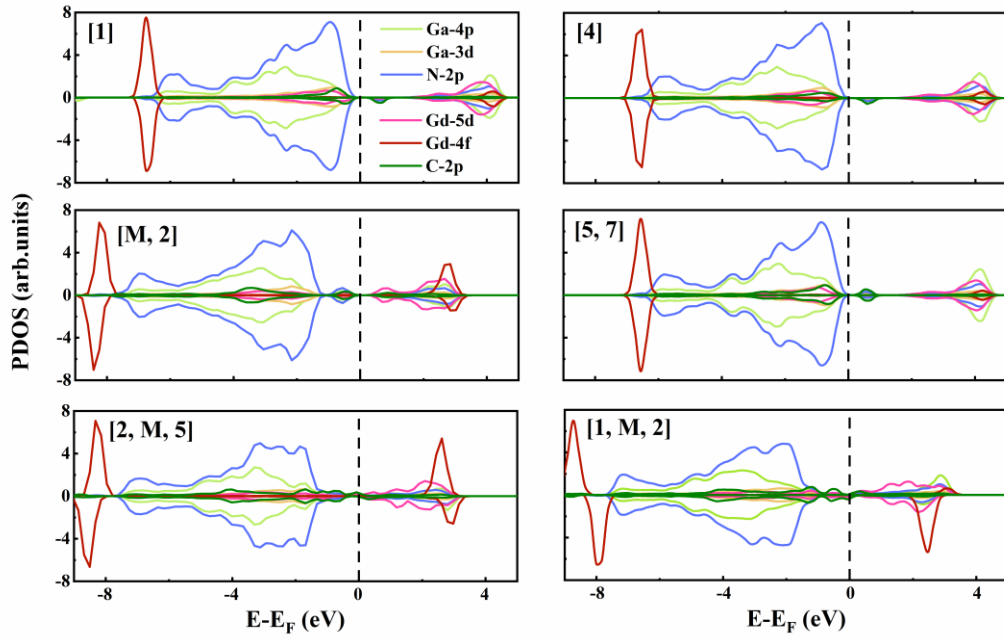


Figure S3. PDOS with AFM states of different substitution site: [1], [4], [M, 2], [5, 7], [2, M, 5] and [1, M, 2].

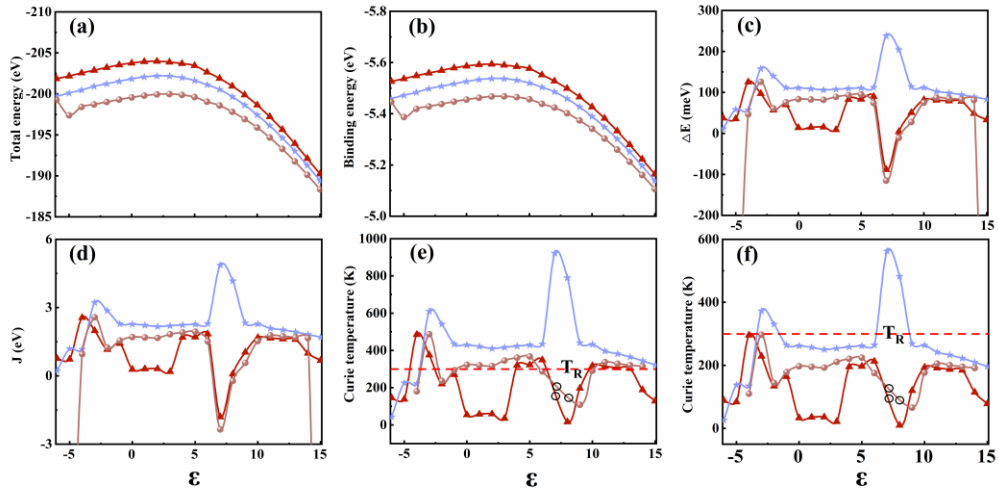


Figure S4. (a) E_{total} of FM phase, (b) E_b , (c) ΔE (d) J , (e) T_C^{FMA} and (f) T_C of $\text{Ga}_{14}\text{N}_{16-n}\text{Gd}_2\text{C}_n$ monolayers computed by the PBE method with SOC. The dark blue (triangle), light blue (pentagram) and brown (circle) lines in the diagram represent $\text{Ga}_{14}\text{N}_{15}\text{Gd}_2\text{C}_1$, $\text{Ga}_{14}\text{N}_{14}\text{Gd}_2\text{C}_2$ and $\text{Ga}_{14}\text{N}_{13}\text{Gd}_2\text{C}_3$ monolayers, respectively. The black circles in the last two figures indicate this position as an AFM state without T_C .

Table S2. A brief summary of the magnetic properties for doped GaN materials.

Materials	Magnetic type	Magnetic moment	T _C	Ref.
Ga ₃₅ N ₃₆ Mn	FM	4.0 μ_B	-	[5]
Ga ₃₅ N ₃₆ Cu ₂	FM	4.0 μ_B	-	[14]
Ga ₁₆ N ₁₅ Fe	FM	5.0 μ_B	-	
Ga ₁₆ N ₁₅ Co	FM	4.0 μ_B	-	[15]
Ga ₁₆ N ₁₅ Ru	FM	5.0 μ_B	-	
Ga ₁₆ N ₁₅ Dy	FM	5.1 μ_B	-	[19]
Ga ₁₆ N ₁₄ GdSm	FM	12.01 μ_B	-	[20]
CrBr ₃	FM	-	34K	[40]
CrI ₃	FM	-	45K	[41]
Fe ₃ GeTe ₂	FM	-	130K	[42]
CrSe ₂	FM	-	65K	[43]
CrGeTe ₃	FM	-	30K	[44]